Deep inelastic pion-induced nuclear reactions in the isobar model*

J. N. Ginocchio
Theoretical Division, Los Alamos Scientific Laboratory, University of California, Los Alamos, New Mexico 87545
(Received 19 July 1977)

Deep inelastic pion-induced nuclear reactions are calculated in the isobar model, which assumes that an interacting resonant pion and nucleon form an unstable particle, the Δ, which can propagate through the nucleus and either decay or be absorbed by interacting with other nucleons in the nucleus. The propagation of the particles is treated classically and the interactions are assumed to be incoherent. The lifetime of the Δ is taken to be energy dependent as prescribed by measured pion-nucleon scattering and the cross section of the Δ absorption is determined by measured pion production in two nucleon collisions. The formation of the Δ by a pion and nucleon and the subsequent absorption of the Δ provide a two-step mechanism for pion absorption. These calculations indicate that the pion is absorbed mostly on the inside forward edge of the nuclear surface where the nuclear density has almost reached central density. The calculations are compared with measured pion absorption cross sections, proton spectra, and spallation products in pion-induced reactions. All of these data indicate that pion absorption is underestimated in this model by perhaps as much as 35%, particularly for low energy (~100 MeV) pions. Possible explanations for these discrepancies are discussed.

[NUCLEAR REACTIONS Calculated absorption cross section, proton spectra, and spallation products for pion-induced reactions on various nuclei.]

I. INTRODUCTION

Pion reactions with nuclei are of special interest for a number of reasons. One reason is that there are three possible charge states of the pion. Another is that the pion can be absorbed by nuclei giving up its entire rest mass energy to the nucleus. Furthermore, the dominance of the (3,3) resonance for intermediate energy pions gives promise of understanding pion reactions and thus using the pion as a useful probe of nuclei. As a consequence there is a great deal of experimental investigation of pion reactions with nuclei, and a wealth of data is becoming available.

For reactions in which the energy transferred into internal energy of the target is large compared to the binding energy of nucleons in the target, which we shall refer to as deep inelastic reactions, the many-body scattering problem can be approximately formulated strictly in terms of on-shell pion-nucleon and nucleon-nucleon scattering amplitudes. Furthermore, if the mean free path of the incident particle λ is much larger than the de Broglie wave length Λ then the scattered wave will approximately reach its asymptotic value before the next scattering and a classical treatment of the scattering becomes reasonable. If in addition the radius of the target nucleus is large with respect to the mean free path of the projectile then there will be many scatterings inside the nucleus and the interference terms between different scattered waves will tend to cancel out. Finally, if the mean free path is larger than the interparticle distance d, the scattering from different nucleons in the nucleus can be assumed to be approximately independent of each other. Thus if we have

$$\Lambda \ll \lambda \ll R, \tag{1a}$$

$$d \ll \lambda, \tag{1b}$$

then a reasonable approximate approach is to treat the interaction of the incoming particle with the nucleus as a series of independent collisions with the target nucleons, using the free particle-nucleon differential cross sections.[1] The nucleons that are struck can then hit other nucleons as well, and these collisions are likewise treated as independent collisions. A cascade of nucleons moving through the target is thus built up. For this reason this approach has been called the intranuclear cascade model.[2,3] The struck nucleons either leave the nucleus or lose enough energy in subsequent collisions to be trapped by the attraction of the remaining nucleons. After this "fast" stage is finished the nucleus left over is highly excited and will evaporate low energy nucleons and α particles until it reaches a stable nucleus.[4] Both the spectrum of particles emitted and the cross sections of the residual nuclei calculated by this model have been successfully compared with experimental results of deep inelastic reactions induced by nucleons.

For pion reactions with energy in the region of the (3,3) resonance, the pion-nucleon cross sec-

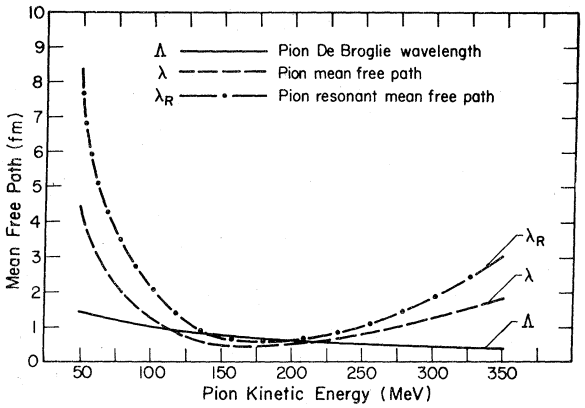

FIG. 1. The pion de Broglie wavelength Λ, the average pion mean free path λ, and the average pion resonant mean free path λ_R are plotted as a function of pion kinetic energy.

tion is very large leading to a short mean free path. In Fig. 1 we have plotted the pion de Broglie wavelength Λ and the pion mean free path

$$\lambda = (\bar{\sigma}_{\pi N}\rho_0)^{-1} \tag{2a}$$

versus incident pion energy, where $\bar{\sigma}_{\pi N}$ is the average pion-nucleon cross section

$$\bar{\sigma}_{\pi N} = \tfrac{1}{2}(\sigma_{p,\pi^+} + \sigma_{n,\pi^+}), \tag{2b}$$

$\rho_0 = 0.17$ fm^{-3}, and we have assumed, for this purpose, that the nucleons have no momentum but have an average kinetic energy $\bar{\epsilon} = \frac{3}{5}\epsilon_F$ where $\epsilon_F = 38$ MeV · MeV, although such simplifications are not made in the intranuclear cascade calculation. We see from Fig. 1 that the mean free path will be comparable to the pion de Broglie wave length and the interparticle distance. Inside the nucleus the mean free path will be increased from these values because of the Pauli principle, but since the pion-nucleon differential cross section is not at all forward-peaked through the resonance region this correction will not be large. Thus condition (1) cannot be satisfied and the intranuclear cascade approach is questionable.

In addition an important part of the pion-nucleus interaction which distinguishes it from the nucleon-nucleus interaction is the fact that the nucleus can absorb the pion and transfer its rest mass (about 140 MeV) and kinetic energy to excitation energy of the nucleus. However, in normal nuclear matter one nucleon cannot absorb a pion without violating energy and momentum conservation. Hence the pion must interact with at least two target nucleons before it can be absorbed.

We shall discuss in this paper a way of modifying the intranuclear cascade approach so that these two objections may be overcome. This discussion is the subject of Sec. II. In Sec. III we shall compare calculations with this model with recent experimental data and try to draw conclusions about the model.

II. ISOBAR MODEL

The reason that the mean free path of the pion is so small is due to the large $l = 1$ pion-nucleon resonant cross section. We shall attempt to turn the existence of the resonance to our advantage. We assume that for the pion-nucleon resonant reaction, which we define precisely in Eq. (8a), the pion and nucleon form an unstable particle, with angular momentum and isospin of $\frac{3}{2}$ which we call the delta (Δ):

$$\pi + N \rightarrow \Delta. \tag{3}$$

The Δ will have, on the average, a smaller de Broglie wave length than the pion since we assume momentum is conserved in the reaction (3), but as we shall see later, its mean free path will be longer than its de Broglie wavelength, and for certain energies, longer than the internucleon distance. Thus the Δ can be treated classically, and condition (1) is satisfied.

After traveling through the nucleus, the Δ can decay back into a pion and nucleon,

$$\Delta \rightarrow \pi' + N_1'. \tag{4}$$

Alternatively the Δ can also collide with a target nucleon before it decays, and in such a collision it can change back into a nucleon *alone*, i.e.,

$$\Delta + N_2 \rightarrow N_1' + N_2'. \tag{5}$$

This type of collision combined with (3) provides a two-step mechanism for pion absorption. In addition (5) also includes some of the interaction of the nucleon in the Δ with the neighboring nucleon and hence, to some extent the collisions are not independent.

Thus by treating the pion-nucleon resonating system as a particle, the pion does not interact independently with the nucleons but the Δ does. We thus have a model which circumvents the objections raised in the Introduction to using the intranuclear cascade for pion-induced reactions.

This isobar model for deep inelastic pion reactions has been developed and used with some success.[5] However, there have been discrepancies reported in the measured proton spectra[6] and spallation[7] results for pion-induced reactions compared with this generalization of the intranuclear cascade. As a result the model has been reexamined and essentially three refinements in the physics have been made. (1) The Δ width, which determines the mean free path for decay of the Δ, is taken to be energy dependent as prescribed by

pion-nucleon phase shift analysis.[8] This is very important since the width varies from 35 MeV for 70 MeV pions to 181 MeV for 350 MeV pions, whereas a constant width of 90 MeV was used previously. (2) The pion is allowed to undergo both nonresonant and resonant scattering. In the original version the Δ was formed in all pion-nucleon collisions. (3) The cross section for a Δ to collide with a nucleon and go to two nucleons, Eq. (3), is calculated in the one-pion exchange model with a form factor.[9] Previously the one-pion exchange cross section was used which overestimates this cross section. We shall discuss these three improvements in more detail in the next three subsections.

We have in this paper ignored other isobars, in particular the $l=0$ isobars which can have both isospin $\frac{1}{2}$ and $\frac{3}{2}$ and which can affect the absorption reaction differently (see Appendix). We may find it necessary to incorporate these as well to completely understand the absorption process.

A. Δ width

The width of the Δ will depend on the center-of-mass three-momentum, t, of the pion. For low t it will increase like t^3 which results from the phase space available to a resonance with an orbital angular momentum equal to unity and for high t it decreases to zero.[10] A simple energy dependence has been determined[8] which fits these constraints and also the pion-nucleon scattering information, and it is given by

$$\Gamma(t)=\Gamma_0(\rho(t)/\rho(t_0)), \tag{6a}$$

where

$$\rho(t)=t^3[1+(R_1t)^2+(R_2t)^4]^{-1} \tag{6b}$$

and

$$\begin{aligned}&\Gamma_0=112\text{ MeV},\\ &t_0=1.15\text{ fm}^{-1},\\ &R_1=0.83\text{ fm},\\ &R_2=0.62\text{ fm},\end{aligned} \tag{6c}$$

and t is in units of inverse femtometers.

The mean free path for decay of the Δ is essentially the velocity of the Δ times its mean lifetime,

$$\lambda_D(t)=\hbar C\beta[\Gamma(t)(1-\beta^2)^{1/2}]^{-1}, \tag{7a}$$

where β is the velocity of the Δ in units of the velocity of light. Using Eq. (6) and the fact that the momentum of the Δ is given by the momentum of the pion plus the nucleon, λ_D will decrease like t^{-2} for t small (pion energy $\leq$350 MeV) increase like t for t large (pion energy $\geq$350 MeV). The fact that the mean free path decreases as the pion energy increases implies that absorption will become less important in the pion reaction cross section as the pion energy increases.

In Fig. 2 we have plotted the average distance for scattering for a resonant pion. This distance is the sum of the average mean free path for decay plus the pion mean free path,

$$\lambda_{DS}=\lambda_D+\lambda_R. \tag{7b}$$

In calculating λ_{DS} we assume that the nucleons are at rest but have a kinetic energy $\bar{\epsilon}=\frac{3}{5}\epsilon_F$ where $\epsilon_F=38$ MeV. We see that this distance is larger than the pion and Δ de Broglie wavelength although through the resonance region it still is smaller than the internucleon distance. However, even though the mean free path is smaller than the internucleon distance, the nucleon inside the Δ interacts with the neighboring nucleon and thus the reason for condition (1a) is approximately fulfilled. Hence the distance gained by allowing the Δ to propagate does alleviate the problems discussed in the Introduction to some extent. In addition the Pauli principle will increase λ_{DS} inside the nucleus. We shall find that greater benefits accrue for the pion absorption channel.

The angular distribution of the pion as it decays from the Δ should in principle be that of a decaying $l=1$, $J=\frac{3}{2}^+$ resonance. However, the total nonresonant plus resonant angular distribution should reproduce the measured pion-nucleon angular distribution. This angular distribution has a term due to the interference of the $l=1$ and $l=0$ partial waves. Since our classical treatment has no way of reproducing this interference we incorporate this into our model by having the angular distribution of both the Δ decay and the nonresonant scattering each be that of the measured angular distribution.

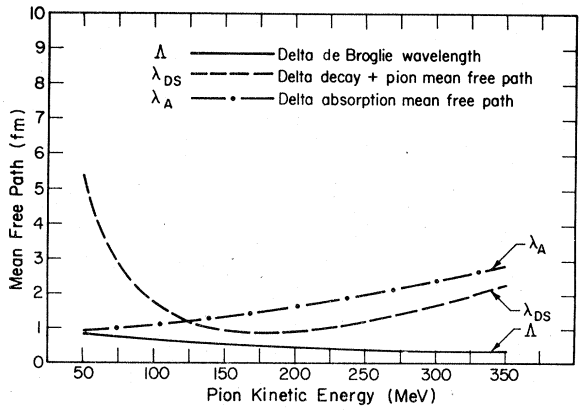

FIG. 2. The Δ de Broglie wavelength Λ, the average Δ creation plus decay mean free path λ_{DS}, and the average Δ absorption mean free path λ_A are plotted as a function of the pion kinetic energy.

In the original version of this isobar model[4] a constant width of 90 MeV was used. For pion energies below 156 MeV the width in Eq. (6) will be smaller than 90 MeV and hence, relatively speaking, the Δ will have more chance of being absorbed, other things being equal. For pion energies above 90 MeV just the opposite is true except for those reactions for which the pion energy decreases below 90 MeV.

B. Resonant cross section

The probability that the pion and nucleon form a Δ is directly proportional to the resonant cross section σ_R, which is assumed to have a relativistic Briet-Wigner form the parameters of which are determined by pion-nucleon scattering data[8]:

$$\sigma_R = \frac{8\pi}{l^2} \frac{\omega_0^2 \Gamma(t)^2}{(\omega^2 - \omega_0^2)^2 + \omega_0^2 \Gamma^2(t)} . \tag{8a}$$

The variable ω is the invariant mass of the pion-nucleon system and is given in terms of t as

$$\omega = \{[m^2 + (\hbar c t)^2]^{1/2} + [M^2 + (\hbar c t)^2]^{1/2}\}, \tag{8b}$$

where m and M are the pion and nucleon masses, respectively, in units of energy, and $\hbar c = 197$ MeV fm. The parameter ω_0 is the value of ω for $t = t_0$ and numerically is

$$\omega_0 = 1.231 \text{ GeV}. \tag{8c}$$

The mean free path for resonant scattering

$$\lambda_R = \frac{1}{\bar{\sigma}_R \rho_0} \tag{8d}$$

is plotted in Fig. 1, where $\rho_0 = 0.17$ fm^{-3}. We see that it is a large part of the pion mean free path λ_π particularly in the resonance region.

The nonresonant cross section is then given by the difference between the measured total pion-nucleon cross sections and the resonant cross section

$$\sigma_{NR} \equiv \sigma - \sigma_R . \tag{9}$$

C. Absorption cross section

The probability for absorption of the Δ and, consequently the pion, is determined by the process Eq. (5). This cross section is calculated in the one-pion exchange model with a phenomenological form factor[9]; the direct and exchange graphs are shown in Fig. 3. The differential cross section in this model is[11]

$$\frac{d\sigma_A}{dz} = \frac{4\pi}{9U^2}\left(\frac{g^2}{4\pi}\right)\left(\frac{\bar{g}^2}{4\pi}\right)\left(\frac{Mp}{\omega\bar{p}}\right) \times [q_1^4 f^2(q_1) + q_2^4 f(q_2) - \tfrac{1}{2} q_1^2 q_2^2 f(q_1) f(q_2) - \tfrac{1}{2}(p^2 - \bar{p}^2)^2 f(q_1) f(q_2)], \tag{10a}$$

where $\bar{p}$ is the center-of-mass three-momentum of the Δ-nucleon system, p the center-of-mass momentum of the nucleon-nucleon system, U is the invariant mass given by

$$U = [M^2 + (\hbar c \bar{p})^2]^{1/2} + [\omega^2 + (\hbar c \bar{p})^2]^{1/2} = 2[M^2 + (\hbar c p)^2]^{1/2}, \tag{10b}$$

q_1 and q_2 are the three-momentum transfer in the direct and exchange scattering, respectively, and are given by

$$q_1^2 + p^2 + \bar{p}^2 - 2p\bar{p}z, \qquad q_2^2 + p^2 + \bar{p}^2 + 2p\bar{p}z, \tag{10c}$$

z is the center-of-mass scattering angle.

The g is the pion-nucleon coupling constant and the value used is[12]

$$\frac{g^2}{4\pi} = 14.0. \tag{10d}$$

The pion-Δ coupling constant is determined by the Δ decay properties[13] and has the value

$$\frac{g^2}{4\pi} = 68.3 \tag{10e}$$

which is very close to the quark model value. The function $f(q)$ is the pion propagator times the form factor $F(q)$,

$$f(q) = F(q)(m^2 + q^2)^{-1}, \tag{10f}$$

where the form factor is given by

$$F(q) = [1 + (q/q_0)^2]^{-1} \tag{10g}$$

and q_0 is a parameter we shall discuss shortly.

The total absorption cross section is given by the integral over the center-of-mass angle

$$\sigma_A = \int_{-1}^{1} \frac{d\sigma_A}{dz}\, dz . \tag{10h}$$

The total cross section determines the probability of absorption and the differential cross section the angle between the two nucleons produced.

The form factor keeps the two nucleons produced in the absorption apart at short internucleon distances. The range parameter q_0 we determine by using the inverse of the reaction as a model for

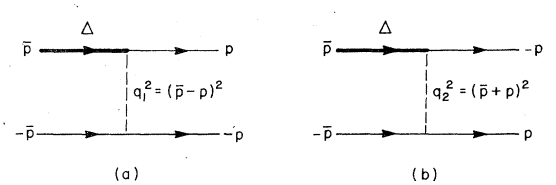

FIG. 3. Direct (a) and exchange (b) diagram for Δ absorption where $\bar{p}$ and p are Δ and final nucleon center-of-mass momenta, respectively.

pion production, that is the inverse of Eq. (5) followed by Eq. (4). We can then compare this result with the experimental proton-proton data on pion production.[14] Of course, in such a collision any invariant mass ω of the pion-nucleon resonant system can be produced within the range

$$\omega_{\min} \leq \omega \leq \omega_{\max}, \tag{11a}$$

where

$$\omega_{\min} = m + M,$$
$$\omega_{\max} = [2M(2M+T)]^{1/2} - M \tag{11b}$$

and T is the incoming nucleon laboratory kinetic energy. $\omega_{\min}$ corresponds to the pion momentum, t, being zero and $\omega_{\max}$ to the Δ momentum, $\bar{p}$, being zero. Using detailed balance and the fact that a resonance of width $\Gamma(t)$ is being produced, the production cross section is[15]

$$\sigma_\pi = \frac{2\bar{p}^2}{p^2}\,\sigma_A W(\omega), \tag{12a}$$

where

$$W(\omega) = \frac{\omega_0 \Gamma(t)}{0.898\pi[(\omega^2 - \omega_0^2)^2 + \omega_0^2\Gamma^2(t)]} \tag{12b}$$

which integrated over all $(T \to \infty)$ gives unity. The total pion production cross section is then given by

$$\sigma_\pi = \int_{\omega_{\min}^2}^{\omega_{\max}^2} \sigma_A(\omega) W(\omega) d\omega^2. \tag{12c}$$

In Fig. 4 we have plotted the experimental one-pion production cross section as a function of proton kinetic energy against the isobar model one-pion cross section as given by Eq. (12c) for various values of q_0 to show the sensitivity to this parameter. The best fit is for $q_0 \approx 513$ MeV/c and this is the value that we have chosen for use in the intranuclear cascade.

However, the comparison indicates that the low-energy pion production is underestimated by this model. Undoubtedly this is due to the fact that the $l=0$ pion-nucleon partial waves are omitted. This is the first sign that these partial waves may play a significant role in pion absorption in the (3,3) resonance region.

Using the average absorption cross section $\bar{\sigma}_A$ we calculate the average absorption mean free path,

$$\lambda_A = \frac{1}{\bar{\sigma}_A \rho_0} \tag{13}$$

and plot λ_A in Fig. 2. We see that the absorption mean free path is larger than the de Broglie wave length of the Δ except for energies below 100 MeV where they become comparable to each other.

D. Propagation of the Δ

In the present calculations we have only included the decay and absorption of the Δ and have not included any scattering of the Δ by nucleons as it propagates through the nucleus, the diagrams show shown in Fig. 5. These cross sections are more open to speculation since there are no experimental data to tie down the magnitude of these cross sections as there is with the decay and absorption cross sections. Hence we have ignored these effects in these calculations in order not to obscure the conclusions we shall draw from comparisons of the calculations with experimental data. However, we are aware of these effects and may find it important to include them in subsequent calculations.

The pion, Δ, and target nucleons all feel an average nuclear potential. Since we explicitly take

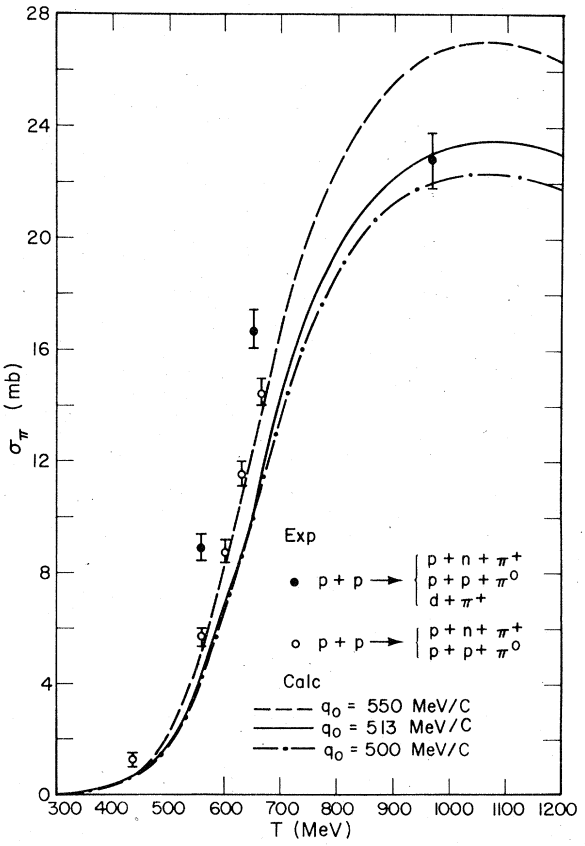

FIG. 4. The experimental and calculated pion production cross section, σ_π, for protons with kinetic energy incident on a proton target. The circles are the measured experimental data taken from Ref. 14. The full circles include $p+p \to d+\pi^+$, whereas the open circles do not. The curves represent the calculation of pion production for three different values of the range parameter q_0 in the form factor.

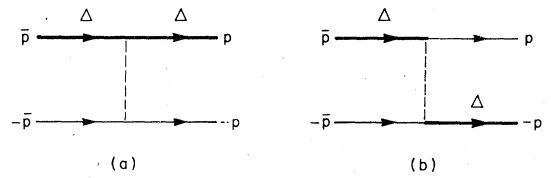

FIG. 5. Direct (a) and exchange (b) diagram for the scattering of a Δ with a nucleon.

into account inelastic scattering, the potential will be a real one. The nucleon potential has been discussed in a number of papers[16] and we use the same potential except for the fact that previously the average measured nucleon separation was used to calculate the potential whereas we use the measured proton and neutron separation energies.

The pion potential is more uncertain and because of the short pion mean free path we have ignored it for this set of calculations, but with the realization that it may be important. The average nuclear potential that the Δ feels is even more uncertain. We take this potential to be the average of the constituent nucleons which depends on the charge of the the Δ. Using the convention that the doubly charged Δ has isospin projection $t_z = \frac{3}{2}$, the Δ potential is taken to be

$$V_\Delta(t_z) = \tfrac{1}{3}(\tfrac{3}{2} + t_z)V_p + \tfrac{1}{3}(\tfrac{3}{2} - t_z)V_n, \qquad (14)$$

where V_p and V_n are the proton and neutron potential, respectively. Both nucleons and Δ's are refracted and reflected by the potential each feels.

As mentioned in the Introduction to this section only the (3,3) isobar has been included in calculations to data. No nucleon-nucleon correlation effects are taken into account.

The remaining details of the intranuclear cascade used are the same as described in many papers[3,5] and will not be repeated in this paper. The multiple scattering is solved using a Monte Carlo technique and the error flags shown on the calculations represent statistical errors in the Monte Carlo procedure.

III. COMPARISON WITH EXPERIMENT

In the next three subsections we shall compare the calculated results of the isobar model with data on pion absorption, proton spectra, and spallation reactions. The central issue will be to determine how well pion absorption in the (3,3) resonance region is explained by introducing the Δ explicitly into the many-body pion-nucleus problem.

A. Pion absorption

The absorption of the pion by the nucleus is a very important part of the reaction of pions with

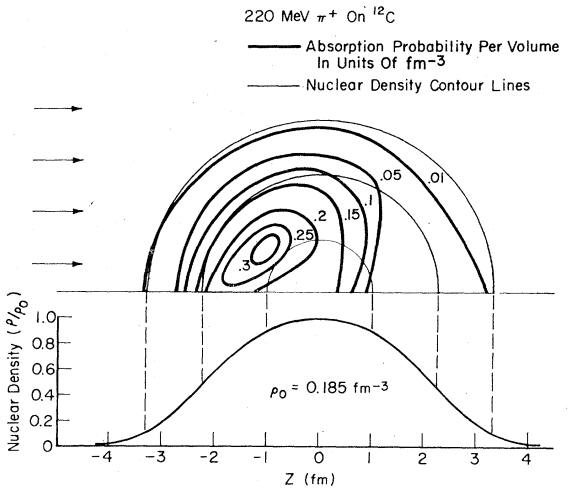

FIG. 6. The absorption probability per volume for 220 MeV π^+ on ^{12}C. The arrows indicate the pion beam incident on the nucleus and define the Z direction with the perpendicular direction defining the impact parameter. The light lines are contour lines of the nuclear density for the upper hemisphere on the nucleus, with the nuclear density defined in the bottom part of the figure. The heavy lines are contour lines for the absorption probability per unit volume in fm^{-3}, normalized so that the integral over the volume is the atomic mass of the target.

nuclei. In Figs. 6 and 7 we illustrate the location in the nucleus at which the pion is absorbed as predicted by the isobar model for 220 MeV π^+ incident on ^{12}C and ^{62}Ni. The arrows refer to the pion beam incident on the nucleus and define the negative Z direction. A cross section of the upper hemisphere of the nucleus is shown with the vertical axes being the x-y plane; the lower hemisphere

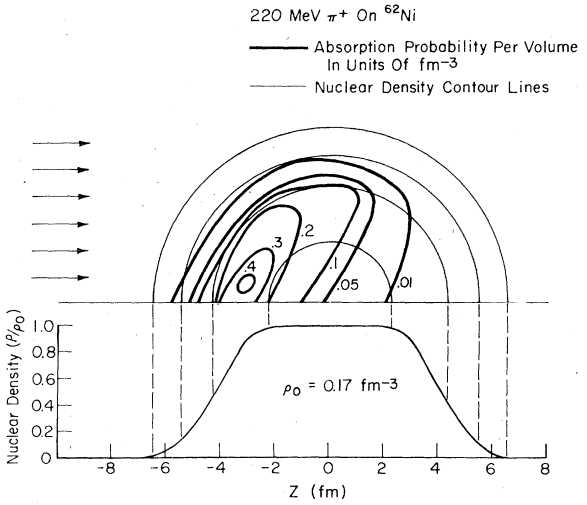

FIG. 7. The absorption probability per volume for 220 MeV π^+ on ^{62}Ni. See caption for Fig. 6 for details.

will just be the mirror reflection of the upper hemisphere. The light circular lines are contour lines for different density regions of the nucleus, the different regions being defined by the lower figure. The heavy dark lines are the contour lines of absorption probability per unit nuclear volume. The normalization is such that the integral of the probability over the nuclear volume is A, the total number of nucleons in the nucleus. For ^{12}C, which is mostly surface, we see that the absorption takes place mostly in the front surface and the interior. For ^{62}Ni, the absorption is mainly on the front surface of the nucleus where the nuclear density is beginning to be constant, and very little absorption takes place in the interior of the nucleus. As a consequence after absorption one or both nucleons will have to traverse a large part of the nucleus.

The absorption distribution does not change significantly for different pion charge. For energies below and above the resonance the pion penetrates deeper into the nucleus before it is absorbed, but this may be a result of the fact that we have neglected the other pion-nucleon partial waves in absorption.

The probability that the pion will charge exchange before it is absorbed varies with energy as well. It increases from 5–8% to 13–18% as the pion energy increases from 100 to 220 MeV, while the probability of double-charge exchange is low at all energies, increasing from less than 1% at 100 MeV to about 2% at 220 MeV.

In Fig. 8 we have plotted the measured and calculated π^+ absorption cross section on ^{12}C as a function of pion energy. The data are a collection of measurements[17,18] from many different groups and is not all of the same quality. In particular for low-energy pions (~50 MeV) there is some ambiguity in the measured value. Nevertheless, on comparing the measured and calculated values we see that the calculated values are consistently 37% lower than the measured values. The experiment may be overestimating the absorption cross section because reactions in which π^0's emerge may may be counted as an absorption event. We have also plotted in Fig. 8 the calculated π^0 cross section plus the absorption cross section and we see that even this falls short of the measured value by about 10%. Hence we conclude that the pion absorption is underestimated by about 10 to 37% by the isobar model.

However, the energy dependence of the absorption cross section is roughly reproduced. The calculated cross section rises rapidly from 50 to 100 MeV and then is relatively flat with pion energy, as is the experimental cross section, although, as we have already mentioned, there is considerable ambiguity near 50 MeV. This flat behavior through the resonance of the magnitude of the absorption cross section is in sharp contrast to the variation in the total reaction cross section through the resonance. Although the total reaction cross section in the resonance region increases, the additional cross section goes into inelastic scattering of the pion rather than into pion absorption. The reason for this is that the pion mean free path becomes so short in the resonance region that although more pions suffer collisions, a lower percentage penetrate into the nucleus to be absorbed. We see this by plotting the ratio of pion absorption to the total pion reaction cross section as a function of energy in Fig. 8. We see that the calculated ratio dips in the resonance region. One experimental ratio at 130 MeV is taken from Ref. 18, while the others are derived from combining pion absorption measurements[17,18] with independent measurements of the total reaction

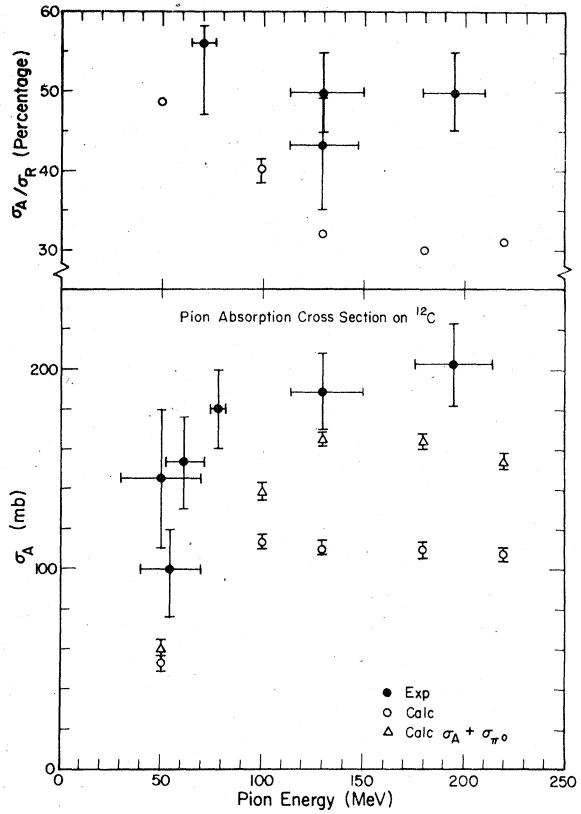

FIG. 8. In the lower graph is plotted the measured pion absorption in ^{12}C, σ_A, from Refs. 17 and 18 (black circles), the calculated values (open circles), and the calculated absorption plus π° cross section (open triangles) versus incident π^+ energy. In the upper graph is plotted the percentage of absorption to total reaction cross section versus incident π^+ energy with experimental values from Ref. 17–19.

cross section.[19] The pion absorption measurements are for π^+ while reaction measurements are for π^-, but these differences have been ignored in light of the large experimental errors. The experimental data are not very good but the ratio does seem to dip as the pion energy increases.

The part of the calculated reaction cross section which is not due to absorption is compared with the experimental values in Table I. Two values for 130 MeV are given using two different sources.[18,19] The experimental errors are large but at least it is clear that there are no large discrepancies between experimental and calculated cross sections as there are for pion absorption. This reaffirms the statement that the treatment of pion absorption is inadequate in the intranuclear cascade model.

In Ref. 18 the conclusion is drawn that about 40% of the pion absorption in ^{12}C is due to absorption on an α particle. This conclusion is based on the number of three-prong events seen in the bubble chamber, that is the number of events for which three charged particles emerge, plus interpretation of some two-prong events as really three-prong events. In order to analyze this statement we compare some of the details of that experiment with our calculated results.

The experiment cannot detect protons with energy less than 12 MeV and cannot distinguish between protons and other charged particles. In the calculations that we present we ignore the contribution of the evaporated charged particles. Hence the cross section for charged particles with energy ≤ 30 MeV will be underestimated in the calculation. As a result the comparison will not be clear cut.

The total percentage of measured two-prong events is 49% compared to a calculated 48%; hence we see that the raw percentages agree. However, the authors interpret 15% of these two-prong events as being associated with a lower-energy undetectable deuteron or proton and hence treat them as being produced by a π^+ impinging on an α particle. Since the calculations imply that if there is another low-energy charged particle, it must come from evaporation, we do not think the absorption on the α-particle interpretation is very solid.

The percentage of measured three-prong events is 23% compared to a calculated percentage of 8% which is a substantial disagreement. Part of the disagreement may come from the fact that one of the measured charged particles may come from evaporation since about 10% of the measured charged particles have low energy. Even so, if we give the benefit of the doubt, at most 15% of the absorption events are three-prong events which cannot be accounted for by the intranuclear cascade. This means that at most 15% of the pion absorption events can be interpreted as absorption on an α particle, as opposed to the 40% quoted by the authors.

A large discrepancy also exists between the number of measured and calculated one-prong and many-prong events. The percentage of measured one-prong events is 12% compared with a calculated 32% and the percentage of measured many-prong events is 15% compared with less than 1% calculated. The inclusion of evaporation may change the calculated percentages so it is difficult to make a firm assessment of the discrepancies. Even if the discrepancies persist, we feel that more basic ingredients in pion-nucleon interactions would be included in the pion-nucleus many-body problem before conclusions are drawn that the absorption takes place on an α particle.

Finally in Fig. 9 we show the variation of the calculated pion absorption cross section with atomic mass of the target of 100 MeV π^+. We see that the absorption cross section grows rapidly, faster than $A^{2/3}$ but less than A.[20] There is a strong dependence on A from the pion absorption distribution portrayed in Figs. 6 and 7. For the lower atomic mass the absorption is spread out in the nucleus implying less chance of absorption. The dependence on energy and charge is very slight. In Fig. 9 we see that the percentage of absorption compared with total reaction cross section has a weak dependence on A. As we have already seen in Fig. 8, there is an energy dependence. Also as the neutron excess increases the percentage of π^- absorption does not rise as rapidly as π^+ absorption. This is due to the fact that π^- cannot be absorbed on a neutron-neutron pair whereas π^+ can.

TABLE I. Nonabsorptive pion-^{12}C reaction cross sections. The first column is the pion energy, the second column is calculated nonabsorptive reaction cross section with absorption cross section subtracted out, and the third column are the experimental values.

T_π (MeV)	$\sigma_R-\sigma_A$ Calc. (mb)	$\sigma_R-\sigma_A$ Exp. (mb)
115–150	231 ± 5	189 ± 20 [a]
		246 ± 26 [b]
180	266 ± 6	230 ± 26 [c]
180–210	239 ± 6	206 ± 26 [d]

[a] Reference 18.
[b] References 18 and 19.
[c] References 17–19.
[d] References 17 and 19.

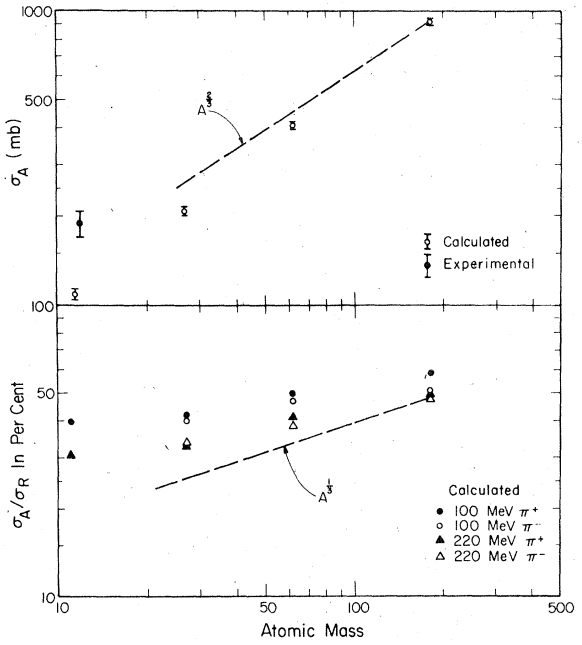

FIG. 9. In the top graph the pion absorption cross section is plotted, σ_A, as a function of atomic mass, the open circles giving the calculated values with statistical error flags, and the full circle the experimental value known only for one mass. The lower curve the ratio of the calculated absorption cross section to total reaction cross in percentage is plotted as a function of atomic mass for various pion charges and energies.

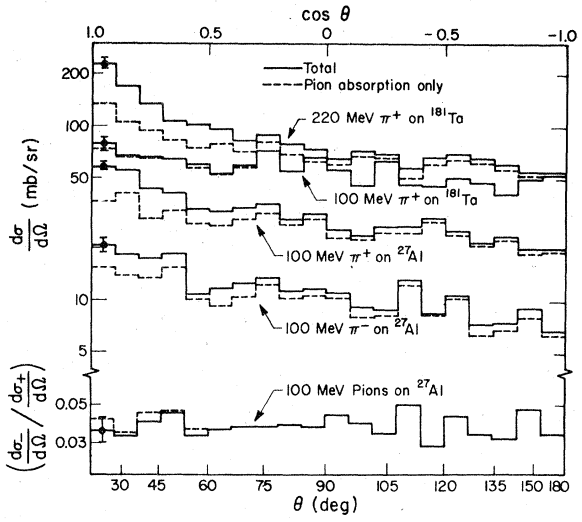

FIG. 10. In the upper graph the differential cross section for proton production $d\sigma/d\Omega$ is plotted versus laboratory angle for various pion energies and targets. The solid histogram gives the proton cross section for all reactions; the dashed histogram the proton cross section for pion absorption only. In the lower graph the ratio of the π^- and π^+ differential cross section for 100 MeV pions on ^{27}Al is plotted versus the laboratory angle.

B. Particle spectra

Reactions in which particles are ejected from the nucleus are generally deep inelastic reactions. Possible exceptions are those reactions in which the residual nucleus is left in a bound state. For pion reactions in the energy range we shall be discussing these latter reactions constitute less than 10% of the particle spectrum. Furthermore, particles emitted at large angles and with large energy will be predominately due to the pion absorption reaction simply because these reactions can deliver more energy to the ejected particles.

In Fig. 10 we have plotted the calculated angular distribution of protons emitted from various pion-induced nuclear reactions (solid histogram) and also the contribution due only to pion absorption (dashed histogram). The evaporation proton spectrum ($E_p \leq 20$ MeV) is excluded from this angular distribution. We see that the dominance of pion absorption varies with mass number and energy. As the energy is decreased from 220 to 100 MeV π^+ on ^{181}Ta the angle above which pion absorption accounts for more than 90% of the emitted protons decreases from 90° to zero. This decrease is due to the fact that low-energy pions have less momentum to impart to the struck proton and also because, as we have seen in Fig. 8, the percentage of pion absorption to reaction cross section increases as energy decreases. For 100 MeV π^+, we see that as the mass of the target increases from ^{27}Al to ^{181}Ta pion absorption plays more of a role for smaller angles. Again this is due to the fact that the percentage of pion absorption increases as the target mass increases. Since the differential cross section due to pion scattering is forward-peaked, while that due to pion absorption is only slightly forward-peaked, the total differential cross section is more forward-peaked for those reactions in which pion absorption plays less of a role.

We also see in Fig. 10 that the π^+ and π^- differential cross sections have the same shape; the ratio of the two cross sections is roughly constant with angle.

The spectrum of protons emitted follow similar trends as seen in Fig. 11. The most energetic nucleons emitted are due to pion absorption. Furthermore, the role of pion absorption for the less energetic nucleons increases as the target mass increases or as the incoming pion energy decreases.

However, the π^+ and π^- spectra for the same energy and target do not have the same shape.

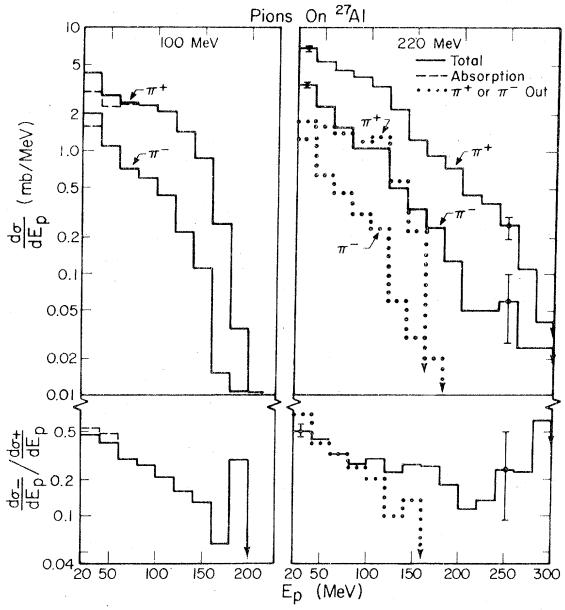

FIG. 11. The top left graph gives the total proton spectrum (solid histogram) for 100 MeV $\pi^{\pm}$ on ^{27}Al as well as that due to absorption only (dashed histogram). The lower left curve gives the ratio of the proton spectra due to π^- and π^+ beams as a function of proton energy E_p. The right-hand curves give the same for 220 MeV pions with the dotted curve being the proton spectrum for which either a π^+ or π^- emerges from the nucleus.

In Fig. 11 we have plotted the ratio

$$R = \frac{d\sigma_-}{dE_p} \Big/ \frac{d\sigma_+}{dE_p} \tag{15}$$

for 100 and 220 MeV pions on ^{27}Al. If the shapes were the same this ratio would be constant as a function of energy. We see that this ratio drops as the energy of the emitted proton increases. For 100 MeV pions it drops monotonically, whereas for 220 MeV pions there is an intermediate proton energy (60–180 MeV) for which this ratio is a constant. We have separated out that part of the 220 MeV proton spectrum for which a π^+ or a π^- emerges (dotted histogram) and we see that the shapes of these spectra are different even for these intermediate energy protons in contrast to the total spectrum.

If the proton struck by the pion left the nucleus immediately, then the π^+ and π^- spectra would have the same shape. Subsequent collisions of the proton with other nucleons may destroy this correspondence. In particular this ratio is sensitive to charge exchange of the outgoing nucleon. We can see this in a simple transport model.[21] However, we emphasize that we have calculated quantitatively all the multiple scattering of the outgoing nucleons explicitly using the measured total and differential nucleon-nucleon cross sections and we only present this simple charge exchange model to give a qualitative understanding of the process.

Using the fact that pion-nucleon interaction is mainly in the isospin $\frac{3}{2}$ state at these energies, the ratio will be given by

$$R_s(E_p) \equiv \left(\frac{d\sigma_-}{dE_p} \Big/ \frac{d\sigma_+}{dE_p}\right)_s = \frac{Z + (9N + 2Z)C(E_p)}{(9Z + 2N) + C(E_p)}, \tag{16a}$$

$$C(E_p) = P(E_p)/Q(E_p), \tag{16b}$$

where the subscript s refers to scattering, that is, those reactions for which the pion is not absorbed, P and Q are the probabilities that the recoil nucleon emerges with and without change of charge, and these probabilities decrease as the nucleon energy increases. We see that for $Z = N$ and $P = Q$ this ratio is unity and decreases to 0.091 as P decreases to zero.

For the protons due to absorption we can derive a similar formula. In the model we have used in the intranuclear cascade, the absorption comes from the formation and subsequent absorption of the Δ [Eq. (3) and Eq. (5)]. In the Appendix we derive a simple expression analogous to Eq. (16) using the isospin properties of this Δ:

$$R_a(E_p) = \left(\frac{Z}{N}\right)\left(\frac{Z + [2Z + 10N(1 + C)]C}{10Z + N + 2NC}\right). \tag{17}$$

Hence for no charge exchange and $N = Z$, $R_a = R_s = 0.091$.

For the same incoming pion energy R_s will vary more dramatically with energy than R_a because absorption will produce higher-energy nucleons for which the charge exchange is less. By the same token for more energetic pions we expect this variation to be less dramatic for both R_s and R_a because higher-energy nucleons are produced and the probability for charge exchange is less. This is the reason for the plateau seen in Fig. 11 in the π^- to π^+ ratio for the 220 MeV pion reactions.

Of course the pion can charge exchange before it is absorbed, which will also affect this ratio. In Tables II and III we illustrate the nature of the two nucleons directly after absorption for 100 and 220 MeV pions on ^{62}Ni. The first column of each table indicates the type of nucleon-nucleon pair produced directly after absorption. The next three columns indicate the fraction of the time that pair is produced by absorption of a π^+, π^0, or π^-, respectively, for π^+-induced

TABLE II. Pion charge exchange before absorption for 100 MeV pions on ^{62}Ni. Column 1 denotes the type of nucleons emerging immediately after absorption. $2p \equiv$ two protons, pn $\equiv$ proton and neutron, $2n \equiv$ two neutrons. Columns 2–6 refer to π^+-induced reactions. Columns 2–4 are the fraction of absorption events for which a π^+, π^0, or π^-, respectively, are absorbed. Columns 5 and 6 are, respectively, the average number of protons and neutrons struck after absorption. Columns 7–11 are as 2–6 but for π^--induced reactions. Column 12 is the ratio of protons produced by π^- to protons produced by π^+ immediately after absorption event. Column 13 is the ratio of protons produced by π^- to those produced by π^+ as the protons emerge from the nucleus.

	π^+					π^-						
	π^+	π^0	π^-	S_p	S_n	π^+	π^0	π^-	S_p	S_n	R_0	R_T
$2p$	0.739	0.008	0.0	1.90	2.83	0.003	0.006	0.0	2.73	2.10	0.15	0.42
pn	0.179	0.052	0.0			0.0	0.042	0.133				
$2n$	0.0	0.019	0.003			0.0	0.011	0.804				

reactions. If there were no pion charge exchange before absorption then the pion absorbed would have the same charge as the incident pion. The next two columns are the average number of protons and neutrons, respectively, which are struck after absorption by the two nucleons. The next five columns give the same information for incident π^- beams. We can see that the pion charge exchanges before being absorbed for about 6–8% of absorption events for 100 MeV pions and about 14–18% for 220 MeV pions. The reason for the increase in charge exchange is that at 220 MeV pions the isospin $\frac{3}{2}$ channel is dominating over the isospin $\frac{1}{2}$ channel and charge exchange in isospin $\frac{3}{2}$ is more likely than in isospin $\frac{1}{2}$.

The next to last column gives the ratio, R_0, of the number of protons produced directly after absorption by π^+. For both energies the ratios are about twice that which would occur if there were no pion charge exchange. In the last column is the ratio, R_T, of the total proton spectrum due to absorption after the protons have emerged from the nucleus, of π^- divided by that due to π^+. We see that this ratio is larger than R_0 for both energies. This implies that the rescattering after absorption, which we see by columns five, six, ten, and eleven is sizable, affects the proton spectra. However, this rescattering is overestimated in this model because we have included refraction of the nucleons as they leave the nucleus. If refraction is ignored the rescattering is reduced by about 35% for 100 MeV incident pions and by about 17% for 220 MeV incident pions.

Fortunately there is extensive proton spectra measured[22] at 100 and 220 MeV pions for two angles $\theta = 45°$ and $\theta = 94°$ and three targets, ^{27}Al, ^{62}Ni, and ^{181}Ta, with which to compare the intranuclear cascade calculations. In subsequent comparisons the $\theta = 94°$ measured spectra are compared with $\theta = 90°$ calculated spectra, the difference in angle being inconsequential given the statistical errors of the calculation. These experiments, which only measure protons with energy above 60 MeV, are very sensitive to the pion absorption mechanism. The calculated proton spectra for 100 MeV pions are, all due to pion absorption, and even for 220 MeV pions, the $\theta = 45°$ spectrum is about 65% due to pion absorption, while the $\theta = 90°$ spectra are about 92% due to pion absorption. In Fig. 12 we show these data, which are measured only for those protons with energy greater than 60 MeV, for 100 MeV pions on ^{27}Al. We see that the overall shapes of the calculated spectra compare well with the measured spectra, but the magnitudes are lower than the measured values particularly for $\theta = 45°$. For π^+ at $\theta = 45°$, the plateau for proton energies between 60–125 MeV and the sharp falloff are

TABLE III. Pion charge exchange before absorption for 220 MeV pions on ^{62}Ni. Columns have same meaning as explained in Table I.

	π^+					π^-						
	π^+	π^0	π^-	S_p	S_n	π^+	π^0	π^-	S_p	S_n	R_0	R_T
$2p$	0.646	0.025	0.0	2.40	3.37	0.012	0.022	0.0	2.76	2.71	0.18	0.42
pn	0.153	0.113	0.005			0.005	0.099	0.112				
$2n$	0.0	0.040	0.019			0.0	0.019	0.732				

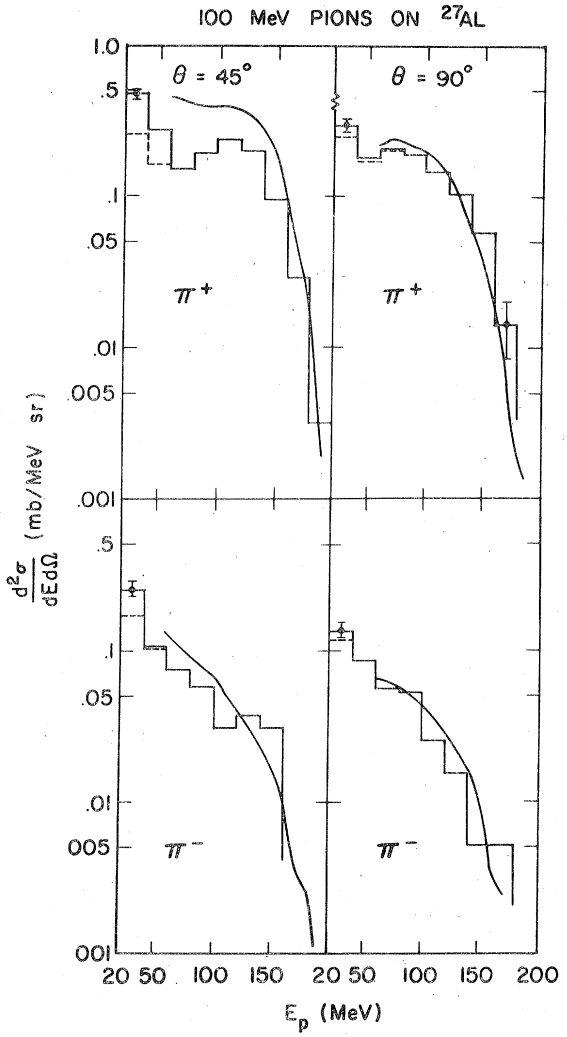

FIG. 12. The double differential proton spectra $d^2\sigma/dEd\Omega$ for two angles with 100 MeV π^+ (upper) and π^- (lower) beams incident on ^{27}Al. The solid histogram is the total calculated proton spectra, the dashed histogram that due to absorption only, the curves are the measured values given in Ref. 21. The measured values are for $\theta = 94°$ instead of $\theta = 90°$ and the error flags indicate statistical errors on the calculations.

reproduced. This spectrum is quite different than the π^--induced spectra at $\theta = 45°$, and the π^+-induced spectra at $\theta = 90°$. These spectra fall off rapidly for proton energies greater than 60 MeV, and this is also reproduced by the calculations.

In Fig. 13 we compare 100 and 220 MeV $\pi^\pm$ on ^{62}Ni at $\theta = 45°$ and 90°. For ease in comparing the π^+ and π^- spectra we have multiplied the π^- spectrum by a factor of 3. We again see that the calculated spectra have similar shapes to the measured spectra, except for the fact that the calculations give many more protons with energy greater than 200 MeV. However, this is not a disagreement because the experimental energy cutoff is 200 MeV protons, and any proton with energy greater than 200 MeV would be counted as a less energetic proton due to the finite thickness of the detector. We notice that the calculated π^+ and π^- spectra are very much alike for protons with energy above 60 MeV, as are the measured spectra, but they do differ at lower energies.

We compare the sum of the proton spectra with energies greater than 60 MeV with the experimental values as a function of A in Fig. 14. We see that not only the magnitude is underestimated but as the atomic mass increases the discrepancy tends to become larger, the amount of this discrepancy depending on energy and angle. The discrepancy in magnitude is the greatest at 100 MeV π^+ at $\theta = 45°$, the calculation giving about 50% less than the measured values. These facts could have three possible reasons, all of which could be true. First of all the Δ propagation is not as simple as we have assumed, the other pion-nucleon partial waves play a role in absorption or some collective pion-nucleus effect is taking place. We shall go into these ideas in more detail at the end of the paper.

The authors of Ref. 22 have used some characteristics of the measured proton spectra to infer that the observed proton spectrum is dominated by primary protons, that is protons that do not suffer any collisions after the pion absorption in the nucleus. We shall examine their reasons in the light of intranuclear cascade model which indicates that the nucleons suffer a number of collisions as they leave the nucleus.

One reason given is that there is very little dependence in the measured π^-/π^+ ratio in the proton spectrum as the atomic mass and neutron excess increase, whereas it may naively be thought that these would effect the ratio if there are many cascades. We see from the simple ratio given in Eq. (17) that the charge-exchange probability in the numerator is multiplied by $10N$ and so is sensitive to the neutron excess. On the other hand, the charge-exchange probability in the denominator is proportional to N^2 and hence these two effects work against each other. In Fig. 15 we plot the calculated ratio against the atomic mass as we see that the intranuclear cascade gives the same weak increase in this ratio as the atomic mass increases as the measured ratios do. Furthermore, the magnitude of the ratio is reproduced well, the exception again being the 100 MeV pion data at 45°.

The other reason given is the fact that except for the 100 MeV, $\theta = 45°$ data, the π^+ and π^- spec-

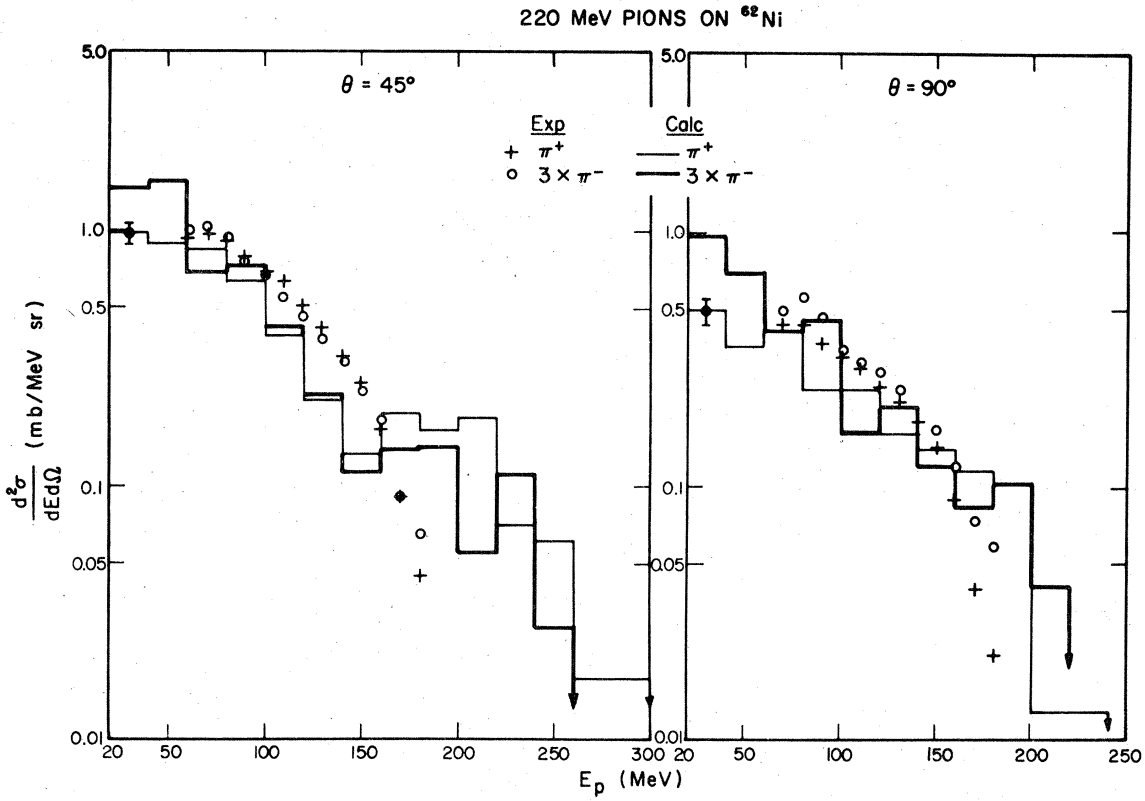

FIG. 13. The double differential proton spectra for 220 MeV pions on ^{62}Ni for $\theta = 45°$ (left) and $\theta = 90°$ (right, with measured values being at $\theta = 94°$). The light solid histogram is the total calculated π^+ induced spectra, the dark histogram is 3 times the π^--induced spectra, the crosses are the measured π^+-induced spectra, and the open circles three times the measured π^--induced spectra (Ref. 21).

tra have the same shape whereas many final collisions would distort the spectrum. While we did note that subsequent collisions do in general distort the spectra, we saw in Figs. 12 and 13, for the particular angles and energy intervals that were measured, the π^+ and π^- spectra are very similar in shape, except for 100 MeV pions at $\theta = 45°$, for which the experimental $\pi^\pm$ spectra disagree in shape as well.

Furthermore, it was stated that the average mean free path of a nucleon with ~100 MeV as determined by optical model analysis of proton elastic scattering data is ~5 fm which would argue that the probability of a collision of an outgoing nucleon would be small. This interpretation is misleading, however, because the elastic scattering takes place near the surface of the nucleus which has a lower density and hence a longer mean free path. Although the calculated pion absorption takes place mainly on the surface, it takes place on two nucleons and there it is very likely that at least one of these nucleons will pass through the interior of the nucleus.

The test as to whether the intranuclear cascade calculates the mean free paths of nucleons correctly is to see how well it reproduces total reaction cross sections for proton-induced reactions.[23] In Fig. 16 we show the reaction cross section calculated for proton-induced reactions as a function of energy for ^{27}Al and ^{208}Pb with and without refraction and reflection included. For ^{27}Al the two calculations bracket the measured cross sections[24,25] and both calculations converge to the measured spectra as the energy increases. For ^{208}Pb the discrepancy is much larger for low energies which indicates the importance of the large Coulomb barrier (~13 MeV) and possible collective effects. However, as energy increases the refraction and reflection calculations converge to the measured reaction cross sections. If the model overestimated the mean free path by say a factor of 4, then the calculated reaction cross sections would be overestimated by a factor of 2 (Ref. 23) which we see is not the case. In fact the bracketing of the measured reaction cross section by the calculation in which refraction and reflection are included and the calculation in which it is not suggests that the treatment of average

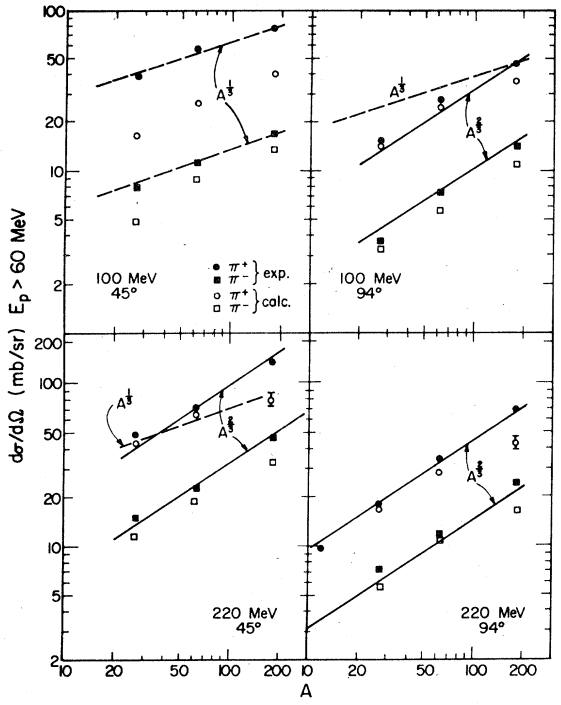

FIG. 14. The cross section for protons emitted with energy greater than 60 MeV for π^+ (measured, Ref. 21, black circles; calculated open circles) and π^- (measured, Ref. 21, black squares; calculated, open squares) plotted versus atomic mass A of the target for 100 and 220 MeV incident pions and protons emitted at two angles, $\theta = 45°$ and 94°.

nuclear field that a nucleon feels may be incorrect in the intranuclear cascade model.[16]

Hence we can only conclude that these features of the data do not warrant the conclusion that the observed nucleons are necessarily primary nucleons since the intranuclear cascade model reproduces these features and certainly has secondary scattering. However, there are severe discrepancies between the measured and calculated magnitudes of the proton spectra, particularly at forward angles and low pion energy, and also between the A dependence of the measured and calculated spectra. But it seems certain that the two nucleons which absorb the pion will suffer some collisions before they leave the nucleus and these will play a role in the complete understanding of these proton spectra.

C. Spallation

The measurement of residual products with mass far removed from the target will be sensitive to pion absorption. In Figs. 17 and 18 we show the calculated cross sections of spallation products of a given atomic mass for 100 and 190 MeV π^+ on copper as a function of the atomic mass of the product. We show as well that part of the cross section which is due to pion absorption only. For 100 MeV $\pi^\pm$ the pion absorption dominates the cross section of nuclei which have 10 or more

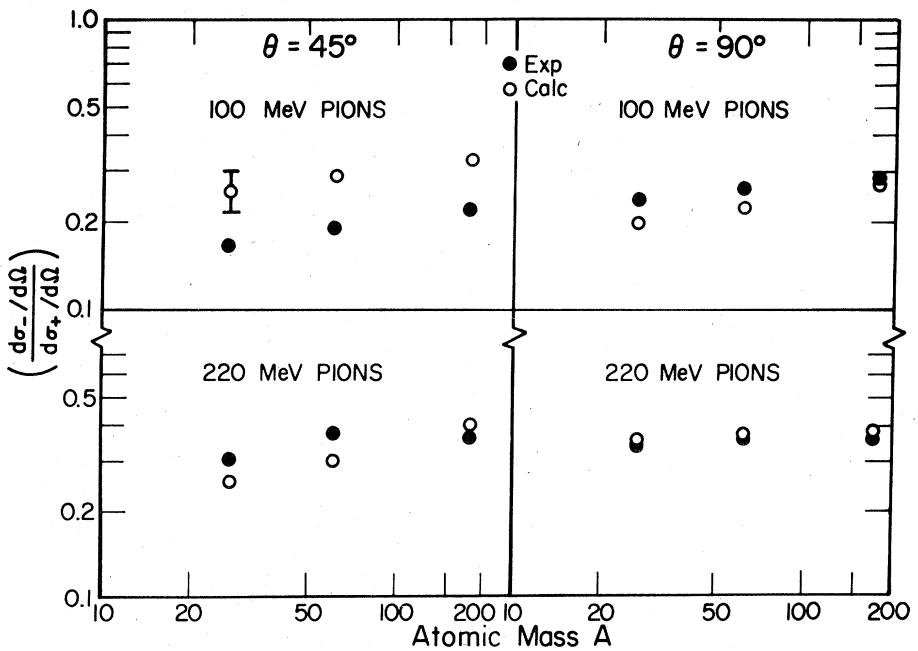

FIG. 15. The ratio of π^- differential proton spectrum for all protons with energy greater than 60 MeV to the π^+ differential cross section for protons with energy greater than 60 MeV as a function of atomic mass. The full circles are the experimental ratios (Ref. 21), with $\theta = 90°$ cross sections being really the $\theta = 94°$ cross sections, and the open circles are the calculated ratios.

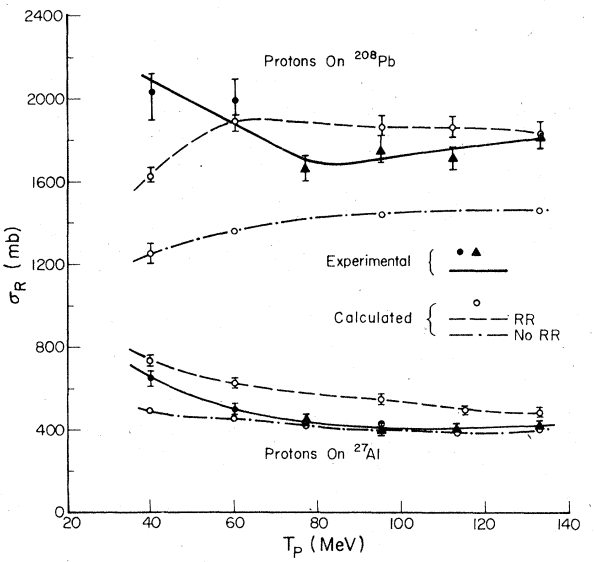

FIG. 16. The reaction cross section σ_R and ^{27}Al and ^{208}Pb as a function of the incoming proton kinetic energy T_p. The open circles are the calculated values, the dash line indicates those calculated with the nucleon allowed to be refracted along its path and reflected at the surface (RR) whereas the dash-dot curve refers to those calculated without refraction and reflection. The solid curves are smooth curves drawn through the measured reaction cross sections with the full circles coming from Ref. 24 and the triangles from Ref. 23.

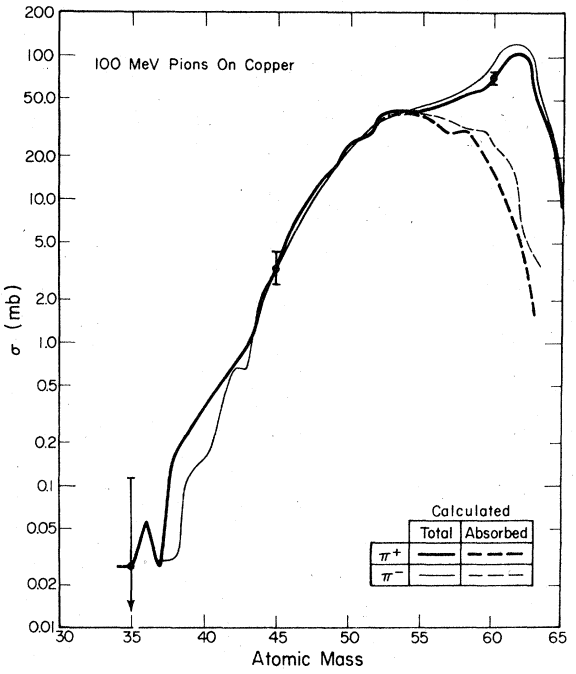

FIG. 17. The total calculated spallation cross section σ, as a function of atomic mass of the product for 100 MeV pions on natural copper. The dark curves refer to π^+-induced spallation, the light curves to π^--induced spallation. The dashed curves refer to the spallation cross section due to pion absorption only.

nucleons removed from the target, whereas for 220 MeV $\pi^\pm$ pion absorption dominates for nuclei which have 15 or more nucleons removed. This is due to the fact that at 100 MeV a greater percentage of the total reaction cross section is due to pion absorption. In addition, less energy is transferred to the nucleus when a 100 MeV pion is absorbed than when a 220 MeV pion is absorbed, thereby producing products closer to the target.

A large part of the calculated spallation yield is due to evaporative processes which takes place after the "fast" intranuclear cascade process. In Fig. 19 we show the distribution of residual nuclei produced by the intranuclear cascade before evaporation for 220 MeV π^+ on ^{62}Ni. The numbers beside the cross section are the average excitation energies in MeV of the residual nuclei. We have also separated out contributions due to absorption only. The residual nuclei produced by scattering are peaked around one nucleon removed from the target and clearly the pion and knocked-out nucleon take away a good fraction (~70%) of the original pion kinetic energy. The residual nuclei produced by absorption are peaked somewhere between two and three nucleons removed from the target and these nucleons take away a similar fraction of the pion rest mass plus kinetic energy. Since there are virtually no residual nuclei produced by the "fast" stage with more than six nucleons removed the evaporation process is responsible for removing most of the nucleons from the target to produce the final spallation products.

A sample of spallation yields have been measured by radiochemical techniques for 100, 190, and 350 MeV $\pi^\pm$ incident on copper.[26] In Fig. 18 we compare these measured yields for 190 MeV $\pi^\pm$ with calculated yields for the same sample of products. We will not attempt to draw conclusions from a detailed comparison of experimental and calculated cross section for each isotope. Rather we shall study more gross features in order to make some conclusions about pion absorption as a function of charge and energy.

The sample of spallation products which are measured represent about 22–30% of the total spallation yield. Also the sample is biased towards neutron deficient isotopes. For π^+ reactions about 94% of the measured cross section is due to neutron deficient isotopes, whereas for π^- about 88% is due to neutron deficient isotopes. This information will be useful in interpreting the results.

In Fig. 20 we plot measured and calculated spallation yields σ_s, the average number of nucleons

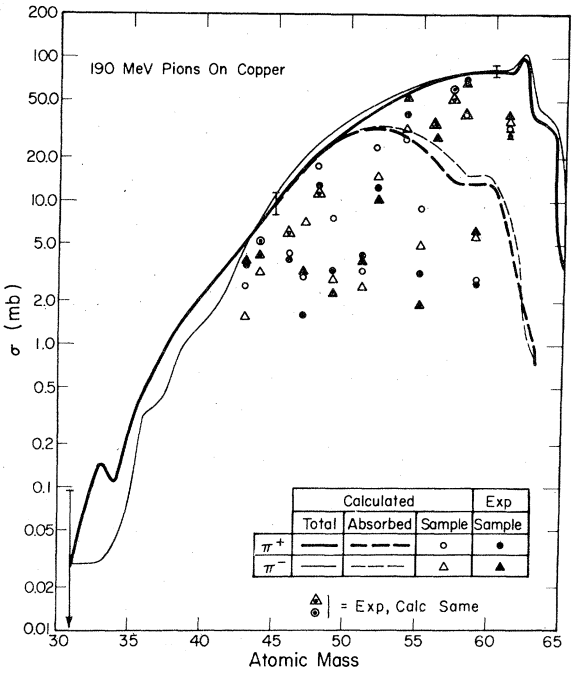

FIG. 18. The curves represent the total calculated spallation cross section σ, as a function of atomic mass of the product for 190 MeV pions on natural copper. The dark curves refer to π^+-induced reactions, the light curves to π^--induced reations. The dashed curves refer to the spallation cross section due to absorption only. The solid circles and triangles refer to the measured sample spallation cross section as given in Ref. 25 for π^+- and π^--induced reactions, respectively, and the open circles and triangles refer to the calculated sample π^+ and π^- spallation cross section, respectively.

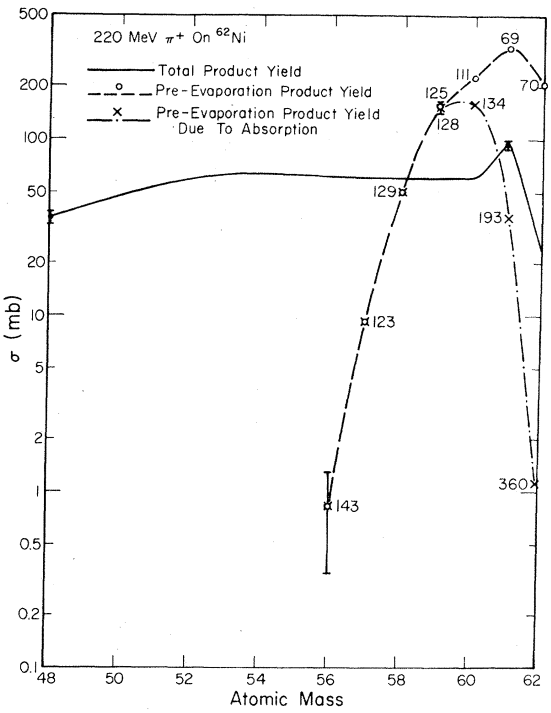

FIG. 19. The solid curve represents the total calculated spallation yield for 220 MeV π^+ on ^{62}Ni as a function of atomic mass of the product. The open circles represent the cross section of a residual nucleus before evaporation with the number beside it being the average excitation energy in MeV of that nucleus. The $\times$'s represent the cross section of a residual nucleus due to absorption only with the number beside it being the average excitation energy in MeV of that nucleus.

removed from the target $\langle \Delta A \rangle$, and the average number of protons removed from the target $\langle \Delta Z \rangle$ versus energy of the incident pion for both negatively and positively charged pions. We define these as

$$\sigma_s = \sum_i \sigma_{s,i}, \tag{17a}$$

$$\langle \Delta A \rangle = \frac{\sum_i (A_0 - A_i)\sigma_{s,i}}{\sigma_s}, \tag{17b}$$

$$\langle \Delta Z \rangle = \frac{\sum_i (Z_0 - Z_i)\sigma_{s,i}}{\sigma_s}, \tag{17c}$$

where $\sigma_{s,i}$ is the cross section for the ith product, Z_i, A_i are the charge and atomic mass of that product, and $Z_0(=29)$, $A_0(=63.6)$ are the charge and atomic mass of the target.

A number of features stand out which are informative. (i) The experimental spallation cross section is consistently underestimated by the model for both charges and all energies. (2) This disagreement becomes worse as the energy decreases. (3) The model underestimates the number of nucleons removed below the (3, 3) resonance and overestimates above the resonance. (4) Generally the discrepancy between the experimental and calculated results is greater for π^- than π^+. (5) The discrepancies are the least near the resonance energy.

Possible explanations for these discrepancies may lie in the fact that only the (3, 3) pion nucleon partial wave is included in the absorption process and the pion potential is ignored. The reasons are as follows. (1) Introducing more partial waves would increase pion absorption and hence increase the spallation cross section. For pion energies below the resonance the pion potential would refract the pion towards the center of the nucleus and thereby increase the possibility of absorption. (2) Pion absorption plays a larger role in spallation as the pion energy is decreased and hence increasing absorption has more of an effect at lower energies. Also refraction of the pion is more

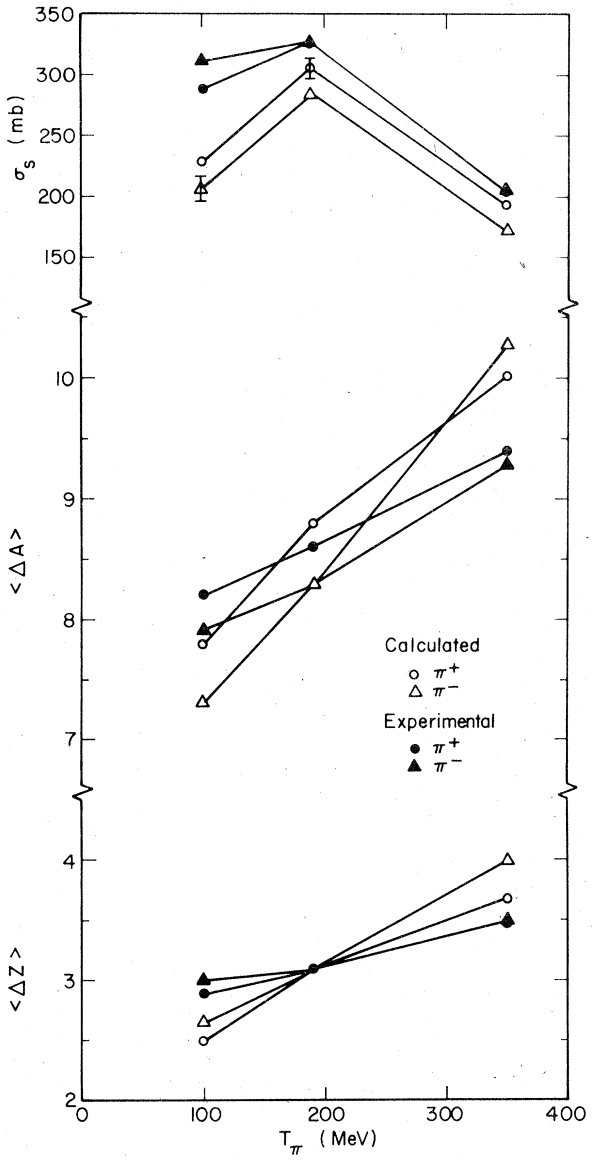

FIG. 20. The top graph is the measured π^+ (full circles) and π^- (full triangles) spallation cross section σ_s, as given in Ref. 25, and the calculated π^+ (open circles) and π^- (open triangles) spallation cross section as a function of pion kinetic energy T_π. Using the same notation the middle and lower graph gives the measured and calculated average number of nucleons and protons removed from the target, respectively, as a function of pion kinetic energy.

important at lower energies. (3) The number of nucleons removed from the target depends on the energy transferred to the nucleus. An increase in pion absorption will increase the average number of nucleons removed which could improve the calculation of $\langle \Delta A \rangle$ below the resonance energy. However, the overestimation of $\langle \Delta A \rangle$ above the resonance is puzzling. (4) For absorption by means of isospin $\frac{1}{2}$ partial waves the residual nuclei produced before evaporation may be closer to the valley of stability than those produced with an isospin $\frac{3}{2}$ isobar (see Appendix). If the introduction of isospin $\frac{1}{2}$ partial waves does shift the products towards the valley of stability, this means that π^--induced reactions will produce more neutron-deficient products, whereas π^+-induced reactions will produce more neutron-rich products. Since neutron-deficient isotopes are primarily the ones measured, the results for π^- will be more affected than the results for π^+. (5) At resonance energy the Δ predominates and the role of other partial waves will be less than below or above the resonance energy.

IV. CONCLUSIONS

The experimental evidence from different types of measurements all indicate that the intranuclear cascade model of pion-induced reactions, in which pion absorption take place through the (3, 3) resonance only, underestimates pion absorption by possibly as high as 35%. The natural question which arises is as follows: Will improvement of the details of the model be able to account for the missing absorption or is a coherent collective effect, which would be outside the scope of the intranuclear cascade model, playing an important role?

The most obvious details of the model which need improvement are the propagation of the pion and the isobar, and the inclusion of other pion-nucleon partial waves in the absorption process. With regard to the propagation of the pion the most significant effect is ignoring the potential the pion feels. Even though the mean free path of the pion is small and hence will feel the potential only over a small distance, the potential will be changing very rapidly and for low-energy pions below the resonance energy will have the effect of bending the pion beam in towards the center of the nucleus and hence increase the probability of absorption. For low-energy proton reactions the refraction of the particle path has been shown to have a substantial effect in the reaction cross section as seen from Fig. 16. For example, for a 40 MeV proton, which has the same momentum as a 170 MeV pion, the reaction cross section is increased by 30% when the nucleons are refracted in the potential and reflected at the nuclear surface.

The effect of a potential on the isobar will be the same because the isobar is made near the nuclear surface and hence feels a changing potential as well. Of course, there is less information about the isobar potential, but the least one can do

is take it as the sum of the pion and nucleon potential.

In addition to the effect of the potential on the isobar there is also the possibility of scattering of the isobar by the nucleons, as indicated in Fig. 5. There are speculations[12,13] but no direct experimental evidence as to what this cross section is. This scattering could increase absorption because the Δ could decrease both its momentum $\bar{p}$, and center-of-mass energy ω, and both of these effects will increase the absorption cross section [see Eq. (10a)]. The charge of the isobar could change as well in this scattering which could effect spallation products produced.

The treatment of the other pion-nucleon partial waves as isobars will definitely increase absorption because there isobars will have an absorption cross section (Fig. 3) as well. For 100 MeV pions the cross section due to other partial waves is only ~10% of the average pion-nucleon cross section but for 350 MeV pions it is ~35%. Absorption of isospin $\frac{1}{2}$ isobars could give a different distribution of spallation products as well (see Appendix). However, the calculated nonabsorptive reaction cross section seems to agree better with the measured values than the absorption cross section, as discussed in Sec. III A, although the data are poor. If this remains to be true as a better reaction cross section data become available, this would imply that it is not sufficient to include other partial waves because this will only increase absorption at the expense of the nonabsorptive reaction cross section. Hence one would need to include the pion potential as well.

Two-nucleon correlations, which we have ignored in these calculations, could be important for pion absorption since the Δ mean free path is comparable to the correlation distance of nucleons in the nucleus. If correlations are important then the interaction of the pion with both nucleons should be treated simultaneously as a three-body problem in order to determine correctly the effect of correlations.

The calculated and measured proton spectra (Fig. 14) disagree more as the incident pion energy decreases and as the target mass increases and the calculated and measured spallation cross section (Fig. 20) disagree more as the incident pion energy decreases. The refinements mentioned will affect these features and may improve the calculated results. However, these features are indicative of a collective coherent process taking place for which the incoherent classical treatment of the Δ would be inadequate. In particular we know that the Δ-hole state is a coherent superposition of many states[27] a fact which is ignored in these calculation tions. We expect such coherent processes to be important for elastic and low inelastic scattering, but they may be important for the deep inelastic reactions that we have discussed in this paper as well. This is of great interest and for this reason it is important to improve the intranuclear cascade model in the ways mentioned and to have more experimental data on the dependence of these reactions on pion energy and target mass.

ACKNOWLEDGMENTS

I wish to thank George Harp for instructing me in the VEGAS intranuclear cascade model which has been the basis of this work, and also Zeev Fraenkel, Gerhart Friedlander, J. M. Miller, and Anthony Turkevich for illuminating discussions of the model. In particular I would like to thank Anthony Turkevich for suggesting the importance of the energy dependence of the Δ lifetime. I thank Bruce Dropesky and Carl Orth for discussions of their copper spallation measurements, and continued enthusiasm about the calculations. I am grateful to Jim Amann, Bob Burman, and John Schiffer for discussions of their measured particle spectra, and particularly to John Schiffer for interesting discussions of the interpretations of these spectra. I thank Ernie Moniz for suggestions concerning the Δ-nucleon absorption cross section, Dick Silbar for discussions of pion transport theory, and Mohan Doss for his bibliography on pion absorption data.

APPENDIX

How does pion absorption on two nucleons depend on the charge states of these nucleons? Since the pion has isospin 1, and the two nucleons can have isospin $T=0,1$, the total isospin of pion plus nucleons can be $I=0,1,2$ with the $I=1$ occurring twice, once each with $T=0$ and $T=1$. In this paper we have assumed that the pion absorption leads to two nucleons; hence $I=2$ will not occur. We denote the amplitude for pion absorption by f_{TI}, with $f_{00}=0$ since the pion cannot couple to zero nuclear isospin to give a total zero isospin.

In this paper we assume that the pion and a nucleon form an isobar first and then this isobar scatters with another nucleon, as shown in Fig. 3. The isobar can have isospin $\tau=\frac{1}{2}$ or $\frac{3}{2}$, although in our calculations we have assumed Δ dominance and have only $\tau=\frac{3}{2}$. If we denote the absorption amplitude in this coupling scheme as $g_{\tau I}$, then clearly these amplitudes are related by an isospin Racah coupling coefficient. In particular for $I=0$ only $\tau=\frac{1}{2}$ can occur and we have

$$f_{10}=g_{1/20}\ . \tag{A1}$$

For $I=1$, writing out the Racah coefficient expli-

citly[28] we have

$$f_{01}=\frac{1}{\sqrt{3}}(\sqrt{2}\,g_{3/2\,1}+g_{1/2\,1}), \tag{A2}$$

$$f_{11}=\frac{1}{\sqrt{3}}(-g_{3/2\,1}+\sqrt{2}\,g_{1/2\,1}). \tag{A3}$$

Hence Δ dominance ($\tau=\frac{3}{2}$ only) implies that there is no absorption for $I=0$, and that absorption by nucleons with zero isospin is twice as likely as nucleon with isospin unity.

The dependence of the absorption amplitude on the charge states of the nucleons will involve linear combinations of these isospin amplitudes using Wigner-3j coefficients. The cross section will depend on the square of this amplitude summed over the individual isospin coordinates of each nucleon in the initial and final state with the constraint that the two nucleons together have initially isospin projection equal to t and the final nucleons have isospin projection $t+p$ where p is the isospin projection of the original pion. When this is done the orthogonality of the Wigner-3j symbols ensures that the absorption is an incoherent sum of the squares of the amplitudes with different T and I:

$$P_a(p,t)=\sum_{T,I,i}(2I+1)\begin{pmatrix}1 & T & I\\ p & t & i\end{pmatrix}^2|f_{TI}|^2, \tag{A4}$$

where $\left(\begin{smallmatrix}abc\\ \alpha\beta\gamma\end{smallmatrix}\right)$ is the Wigner 3-j symbol. Writing out explicitly the 3-j symbol this probability becomes

$$P_a(p,t)=|f_{10}|^2\delta_{p,-t}+|f_{01}|^2\delta_{t,0}+(-1)^t(2t+p)(t-p)(2|t|+2)^{-1}|f_{11}|^2. \tag{A5}$$

We can now determine the ratio of protons produced by π^- and π^+ beams assuming the two nucleons come directly out of the nucleus without scattering. The absorption of π^- ($p=-1$) on two protons ($t=1$) will produce one proton and one neutron and on a neutron-proton pair ($t=0$) will produce no protons. Absorption of a π^+ ($p=1$) on two neutrons ($t=1$) will produce one proton and on a neutron-proton pair will produce two protons. Hence we will have

$$R_a(\text{no rescattering})=\frac{Z^2}{yNZ+N^2}, \tag{A6}$$

where

$$y=6(2|f_{01}|^2+|f_{11}|^2)/(2|f_{10}|^2+3|f_{11}|^2) \tag{A7}$$

and N, Z are the number of neutrons and protons, respectively

The quantity y has a direct physical significance in that it measures to what extent absorption by π^+ and π^- are similar. That is, it measures the extent to which absorption takes place on an n-p pair as opposed to a n-n pair for π^+ and p-p pair for π^-. For y large the $\pi^\pm$ absorption will lead to similar isotopes. For y small the π^+ absorption will tend to produce isotopes more neutron-deficient than those produced by π^- absorption.

For Δ dominance, that is absorption through a $\tau=\frac{3}{2}$ partial wave only, y has a unique value independent of the magnitude of the absorption, $y=10$. Hence for $N=Z$, $R_a=\frac{1}{11}$ and for $N>Z$ it is even smaller. Of course, rescattering will change this ratio considerably, as discussed in the text, and a simple charge exchange model will modify (A6) to give Eq. (17) in the text.

The introduction of $\tau=\frac{1}{2}$ partial waves can change y in either direction depending on the relative magnitude of the $I=0$ and $I=1$ amplitudes. As y increases π^- absorption will produce more neutron-rich isotopes, whereas π^+ absorption will produce more neutron-deficient nuclei.

As we can see from (A2), (A3), and (A4), the absorption process is not incoherent with respect to the partial waves of different isospin τ. The intranuclear cascade as normally practiced would only give the incoherent contribution of the isobars and not the cross terms. Hence some ingenuity would be needed in order to incorporate this coherence in the intranuclear cascade with many pion-nucleon partial waves.

---

*Work performed under the auspices of the U. S. Energy and Development Administration.

[1]M. L. Goldberger and K. M. Watson, *Collision Theory* (Wiley, New York, 1964), Chap. 11, pp. 679–674.

[2]N. Metropolis, R. Bivins, M. Storm, A. Turkevich, J. M. Miller, and G. Friedlander, Phys. Rev. 110, 204 (1958).

[3]K. Chen, Z. Fraenkel, G. Friedlander, J. R. Grover, J. M. Miller, and Yshimamoto, Phys. Rev. 166, 949 (1968).

[4]L. Dostrovsky, Z. Fraenkel, and G. Friedlander, Phys. Rev. 116, 683 (1959).

[5]G. D. Harp, K. Chen, G. Friedlander, Z. Fraenkel, and J. M. Miller, Phys. Rev. C 8, 581 (1973).

[6]J. F. Amann, P. D. Barnes, M. Doss, S. A. Dytman, R. A. Eisenstein, J. Penkrot, and A. C. Thompson, Phys. Rev. Lett. 35, 1066 (1975).

[7]J. Hudis, G. D. Harp, B. J. Dropesky, A. E. Norris, C. J. Orth, and R. A. Williams, Los Alamos Scientific Laboratory Report No. LA-UR-75-875, 1975 (unpublished).

[8]A. Rittenberg, A. Barbow-Goltieri, T. Lasinshi, A. H. Rosenfeld, T. G. Trippe, M. Roos, C. Bricman, P. Soding, N. Borash-Schmidt, and C. G. Wohl, Rev. Mod. Phys. 43, 5114 (1971).

[9]E. Ferrari and F. Selleri, Nuovo Cimento 27, 1450

(1962).
[10]S. D. Drell and F. Zachariasen, Phys. Rev. 119, 463 (1960).
[11]E. Moniz (private communication).
[12]G. E. Brown and W. Weise, Phys. Rep. 22, 279 (1975).
[13]S. Jena and L. S. Kisslinger, Ann. Phys. (N.Y.) 85, 251 (1974).
[14]B. S. Neganov and O. V. Savchenko, Zh. Eksp. Teor. Fiz. 32, 1265 (1957) [Sov. Phys.-JETP 5, 1033 (1957); Yu. D. Prokoshkin, and A. Tiapkin, Zh. Eksp. Teor. Fiz. 32, 750 (1957) [Sov. Phys.-JETP 5, 618 (1957)]; D. V. Bugg, A. J. Oxley, J. A. Zoll, J. G. Rushbrooke, V. E. Barnes, J. B. Kinson, W. P. Dodd, G. A. Doran, and L. Riddiford, Phys. Rev. 133, B1017 (1964), B. Baldoni, S. Focardi, H. Hromadnik, L. Monari, F. Saporetti, S. Femino, F. Mezzanares, E. Bertolini, G. Gialanella, Nuovo Cimento 26, 1376 (1962); T. H. Fields, J. G. Fox, J. A. Kane, R. A. Stallwood, and R. B. Sutton, Phys. Rev. 109, 1713 (1958); R. A. Stallwood, R. B. Sutton, T. H. Fields, J. G. Fox, and J. A. Kane, *ibid.* 109, 1716 (1958); V. M. Guzhavin, G. K. Kliger, V. Z. Kolganov, A. V. Lebedev, K. S. Marish, Yu. D. D. Prokoshkin, V. T. Smolyankin, A. P. Sokolov, L. M. Soroko, and T. Wa-Chuang, Zh. Eksp. Teor. Fiz. 46, 1245 (1964) [Sov. Phys.-JETP 19, 847 (1964).
[15]J. D. Jackson, Nuovo Cimento 34, 1645 (1965).
[16]K. Chen, G. Friedlander, and J. M. Miller, Phys. Rev. 176, 1208 (1968).
[17]R. Salukvadze and D. Neagu, Zh. Eksp. Teor. Fiz. 41, 78 (1961) [Sov. Phys.-JETP 14, 59 (1962)]; M. P. Balandin, O. Ivanov, V. Moiseenko and G. Sokolov, Zh. Eksp. Teor. Fiz. 46, 415 (1964) [Sov. Phys.-JETP 19, 279 (1964)]; H. Byfield, J. Kessler, and L. M. Lederman, Phys. Rev. 86, 17 (1952); J. V. Laberrigue-Frolova, M. P. Balandin, and S. Z. Otvinovskiĭ, Zh. Eksp. Teor. Fiz. 37, 634 (1959) [Sov. Phys.-JETP 10, 452 (1960); N. I. Petrov, V. G. Ivanov, V. A. Rusakov, Zh. Eksp. Teor. Fiz. 37, 957 (1959) [Sov. Phys.-JETP 10, 682 (1960)].
[18]E. Bellotti, D. Cavalli, C. Matteuzzi, Nuovo Cimento 18A, 75 (1973).
[19]F. B. Binon, P. Duteil, J. P. Garron, J. Gorres, L. Hugon, J. P. Peigneux, C. Schmit, M. Spighel, and J. P. Stroot, Nucl. Phys. B17, 168 (1970).
[20]J. Hüfner, Phys. Rep. 21C, 1 (1975).
[21]P. Varghese, R. R. Silber, M. M. Sternheim, Phys. Rev. C 14, 1893 (1976).
[22]H. E. Jackson, S. B. Kaufman, L. Meyer-Schützmeister, J. P. Schiffer, S. L. Tabor, S. E. Vigdor, J. N. Worthington, L. L. Rutledge, R. E. Segal, R. L. Burman, P. A. M. Gram, R. P. Redwine, and M. A. Yates, Phys. Rev. C 16, 730 (1977).
[23]J. Ginocchio and M. Blann, Phys. Lett. 68B, 405 (1977).
[24]R. Goloskie and K. Strauch, Nucl. Phys. 29, 474 (1962).
[25]J. J. H. Menet, E. E. Gross, J. J. Malanify, and A. Zucker, Phys. Rev. C 4, 1114 (1971).
[26]C. J. Orth, B. J. Dropesky, and R. A. Williams, Bull. Am. Phys. Soc. 22, 526 (1977); LAMPF Quarterly Report ending January 31, 1977, Los Alamos Scientific Laboratory Report No. LA-6819-PR (unpublished), p. 86.
[27]E. Moniz, *Meson-Nuclear Physics*-1976, AIP Conference Proceedings No. 33 (American Institute of Physics, New York, 1976), p. 105.
[28]M. Rotenberg, R. Bivins, N. Metropolis, and J. K. Wooten, *The 3-j and 6-j SYMBOLS* (The Technology Press, Cambridge, Maryland, 1959).